◆ Human Brain Mapping 35:6049–6066 (2014) ◆

Atypical Resting Synchrony in Autism Spectrum Disorder

Annette X. Ye,[1,2,3]* Rachel C. Leung,[1,3,4] Carmen B. Schäfer,[1,5] Margot J. Taylor,[1,2,3,4,6,7] and Sam M. Doesburg[1,2,3,4,6]

[1]*Diagnostic Imaging, Hospital for Sick Children, Toronto, Ontario*
[2]*Institute of Medical Science, University of Toronto, Toronto, Ontario*
[3]*Neurosciences and Mental Health, Hospital for Sick Children Research Institute, Toronto, Ontario*
[4]*Department of Psychology, University of Toronto, Toronto, Ontario*
[5]*Institute of Anatomy and Cell Biology, University of Heidelberg, Germany*
[6]*Department of Medical Imaging, University of Toronto, Toronto, Ontario*
[7]*Department of Paediatrics, University of Toronto, Toronto, Ontario*

Abstract: Autism spectrum disorder (ASD) is increasingly understood to be associated with aberrant functional brain connectivity. Few studies, however, have described such atypical neural synchrony among specific brain regions. Here, we used magnetoencephalography (MEG) to characterize alterations in functional connectivity in adolescents with ASD through source space analysis of phase synchrony. Resting-state MEG data were collected from 16 adolescents with ASD and 15 age- and sex-matched typically developing (TD) adolescents. Atlas-guided reconstruction of neural activity at various cortical and subcortical regions was performed and inter-regional phase synchrony was calculated in physiologically relevant frequency bands. Using a multilevel approach, we characterized atypical resting-state synchrony within specific anatomically defined networks as well as altered network topologies at both regional and whole-network scales. Adolescents with ASD demonstrated frequency-dependent alterations in inter-regional functional connectivity. Hyperconnectivity was observed among the frontal, temporal, and subcortical regions in beta and gamma frequency ranges. In contrast, parietal and occipital regions were hypoconnected to widespread brain regions in theta and alpha bands in ASD. Furthermore, we isolated a hyperconnected network in the gamma band in adolescents with ASD which encompassed orbitofrontal, subcortical, and temporal regions implicated in social cognition. Results from graph analyses confirmed that frequency-dependent alterations of network topologies exist at both global and local levels. We present the first source-space investigation of oscillatory phase synchrony in resting-state MEG in ASD. This work provides evidence of atypical connectivity at physiologically relevant time scales and indicates that alterations of functional connectivity in adolescents with ASD are frequency dependent and region dependent. *Hum Brain Mapp 35:6049–6066, 2014.* © 2014 Wiley Periodicals, Inc.

Key words: autism spectrum disorder; resting-state; neural oscillations; functional connectivity; magnetoencephalography; graph theory; developmental cognitive neuroscience; phase synchrony; social cognition.

Additional Supporting Information may be found in the online version of this article.

Contract grant sponsor: Canadian Institutes of Health Research (to MJT); Contract grant number: MOP-119541

*Correspondence to: Annette X. Ye; Diagnostic Imaging, Hospital for Sick Children, 555 University Avenue, Toronto, ON Canada M5G 1X8, E-mail: annette.ye@sickkids.ca

Disclosure: All authors reported no competing financial interests or potential conflicts of interest.

Received for publication 23 September 2013; Revised 3 July 2014; Accepted 28 July 2014.

DOI: 10.1002/hbm.22604
Published online 13 August 2014 in Wiley Online Library (wileyonlinelibrary.com).

INTRODUCTION

Autism spectrum disorder (ASD) is a complex neurodevelopmental disorder characterized by impairments in social communication and social interaction, in addition to restricted, repetitive and stereotyped patterns of behaviors, interests, and activities [APA, 2013]. Increasingly, ASD is understood to be associated with aberrant functional brain connectivity, indicating abnormal coordination of activity among brain regions [Belmonte et al. 2004; Just et al. 2004; Minshew and Keller, 2010; Muller et al. 2011; Schipul et al. 2011; Uhlhaas and Singer, 2007]. Prevailing hypotheses purport that ASD is characterized by reduced long-range functional connectivity and increased local functional connectivity [Belmonte et al. 2004; Courchesne and Pierce, 2005; Minshew and Williams, 2007; Rubenstein and Merzenich, 2003].

Synchronous oscillations represent a core mechanism for sculpting temporal coordination of neural activity across brain-wide networks [Wang, 2010]. Neural synchrony is responsible for coordination and communication between neural populations that are simultaneously engaged in cognitive processes [Fries, 2005; Uhlhaas et al. 2009; Wang, 2010]. Electroencephalography (EEG) and magnetoencephalography (MEG) allow the measurement of electrophysiological signals on a millisecond timescale, which is critical for measuring activity in numerous neurophysiologically relevant frequency ranges [Havenith et al. 2011]. Moreover, as magnetic fields are undisturbed by tissue inhomogeneities, MEG offers the conferred advantage of enhanced localization accuracy and improved oscillatory detectability compared with EEG [Kaiser and Lutzenberger, 2005], providing an ideal modality for imaging oscillatory coherence in distributed brain networks [Palva and Palva, 2012].

Despite numerous empirical studies indicating altered functional brain connectivity in ASD using resting-state functional magnetic resonance imaging [fMRI; see Dichter, 2012; Minshew and Keller, 2010; Vissers et al. 2012 for reviews], only a handful have used resting-state MEG to study connectivity in ASD populations [Cornew et al. 2012; Ghanbari et al. 2013; Pérez Velázquez et al. 2013; Pollonini et al. 2010; Tsiaras et al. 2011]. Findings have largely supported the idea of long-range underconnectivity in the ASD population, although discrepancies in frequency-dependence exist. To date, no study has examined source-space phase synchrony during resting-state MEG in ASD. Accordingly, knowledge remains scant regarding the involvement of specific brain regions and networks in atypical oscillatory synchrony in ASD. Here, we used atlas-guided source reconstruction of MEG data, together with the weighted phase lag index [wPLI; Vinck et al. 2011] and graph theoretical approaches [Rubinov and Sporns, 2010; Zalesky et al. 2010] to investigate resting-state neurophysiological interactions among brain regions in adolescents with ASD.

METHODS AND MATERIALS

Participants

Data were recorded from a total of 20 adolescents with ASD and 15 typically developing (TD) controls. Four ASD participants were removed from the analysis due to excessive movement during recording, resulting in a final sample size of 16 ASD participants (14 males, range = 12–15 years, 14.4 ± 1.1 years, all right-handed) and 15 TD participants (13 males, range = 12–15 years, 14.9 ± 0.9 years, all right-handed). Participants were recruited through the Hospital for Sick Children's Research4kids database and flyers posted in the Greater Toronto Area. Individuals with metal implants, a history of neurological or neurodevelopmental disorders (other than ASD for participants in the clinical group), or IQ $\leq$ 65 were excluded. All ASD participants had a prior clinical diagnosis, which was confirmed using expert clinical judgment and/or the Autism Diagnostic Observation Schedule-General [Lord et al. 2000]. Full scale IQ was estimated for all participants using the Wechsler Abbreviated Scale of Intelligence, consisting of the Vocabulary and Matrix Reasoning subtests [Wechsler, 1999]. All participants and their legal guardians provided written consent for the protocol approved by the Hospital for Sick Children Research Ethics Board and the Declaration of Helsinki.

Data Acquisition

Participants were instructed to maintain visual fixation on a centrally presented gray cross inside a white circle on the screen while remaining still, relaxed and awake in supine position inside a magnetically shielded room. Five minutes of MEG activity was acquired at 600 Hz sampling rate with a band-pass filter of 1–150 Hz and third-order spatial gradient noise cancellation, using a CTF Omega 151 channel whole head system (CTF Systems Inc., Port Coquitlam, Canada). Throughout data acquisition, head position was recorded continuously by measuring the position of the three fiducial coils, located at the nasion and left and right preauricular points. Fiduciary head coils were energized at 1,470 Hz, 1,530 Hz, and 1,590 Hz. Participants with head movement less than 10 mm for 90% of the recording time were considered acceptable for further analysis. This standard of movement tolerance is typical in MEG studies of pediatric populations, allowing collection of MEG data from a clinical child population without creating a biased sample [Taylor et al. 2011]. Median head displacement during the 5-minute recording did not differ between groups ($P > 0.05$).

Following the MEG recording, anatomical MRI scans were acquired for each participant using a 3T MR scanner (MAGNETOM Tim Trio, Siemens AG, Erlangen, Germany). T1-weighted magnetic resonance images were obtained using a high resolution 3D MPRAGE sequence (TR/TE/flip angle = 2,300/2.96 ms/9°, FOV = 28.8 × 19.2 cm, 256 × 256 matrix, 192 slices, slice thickness = 1.0 mm^3 isotropic voxels) with a 12-channel head coil. To support source reconstruction of MEG activity, the anatomical MRI and MEG data were coregistered using fiducial references.

Data Analysis

A flowchart presenting an overview of data processing and analysis pipeline is depicted in Supporting Information Figure S1.

Atlas-guided source reconstruction

We used a scalar beamformer [Cheyne et al. 2006] to reconstruct broadband time series for sources in the brain for 300 seconds of recorded data from each subject. Beamformer analysis affords protection against ocular and nonocular artifacts in MEG imaging [Cheyne et al. 2007]. A time series was computed for each of the 90 cortical and subcortical regions represented in the Automated Anatomical Labeling (AAL) atlas [Tzourio-Mazoyer et al. 2002] (Fig. 1, Supporting Information Table S1). The AAL atlas provides coverage of the whole cortex as well as subcortical areas and has been employed effectively in investigation of brain networks using fMRI [He et al. 2009; Liao et al. 2010; Supekar et al. 2008; Wang et al. 2009] as well as in MEG studies [Diaconescu et al. 2011; Papanicolaou et al. 2006; Tewarie et al. 2013; van Dellen et al. 2013].

Next, broadband time series representing each of the 90 analyzed brain regions were filtered into six bandwidths for further analysis, concordant with classic electrophysiological divisions: δ (1–4 Hz), θ (4–7 Hz), α (8–14 Hz), β (15–30 Hz), low γ (30–80 Hz), and high γ (80–150 Hz). The stop and pass bands of the high-pass filters, and the pass and stop bands of the low-pass filters, respectively, were as follows (in Hz) : δ (0.1, 1; 4, 5), θ (3, 4; 7, 8), α (7, 8; 14, 15), β (14, 15; 30, 31), low γ (29, 30; 80, 81), and high γ (79, 80; 150, 151). The choice of these frequency bands was based on considerable evidence supporting the view that neural oscillations in these bandwidths—and their synchronization—emerge from different neurophysiological mechanisms and play distinct roles in cortical computation and cognition [see Wang, 2010 for review].

Multilevel network characterization

To investigate whether functional connectivity was altered in adolescents with ASD, and to describe group differences in dynamic relations between spatial and functional organization of regional clusters in the brain, we used a multilevel approach which aimed to characterize atypical connectivity using bivariate statistics and graph theory. First, we estimated inter-regional functional connectivity by measuring phase synchrony between the time series of each possible pair of sources. Then, we characterized large-scale lobar differences in functional connectivity by sorting each source into an anatomical subgroup (lobe) and contrasting the two groups of adolescents. Next, nonparametric testing was applied to investigate network-level connectivity as a function of the number of contiguously interconnected nodes between which the extent of connectivity was different between groups [network-based statistic (NBS); Zalesky et al. 2010]. Finally, we quantified graph measures in each frequency at the "whole network" level in addition to performing multivariate analysis of these network measures at the level of each node/region. Taken together, these analysis approaches provide complementary accounts of alterations in resting network synchrony in adolescents with ASD.

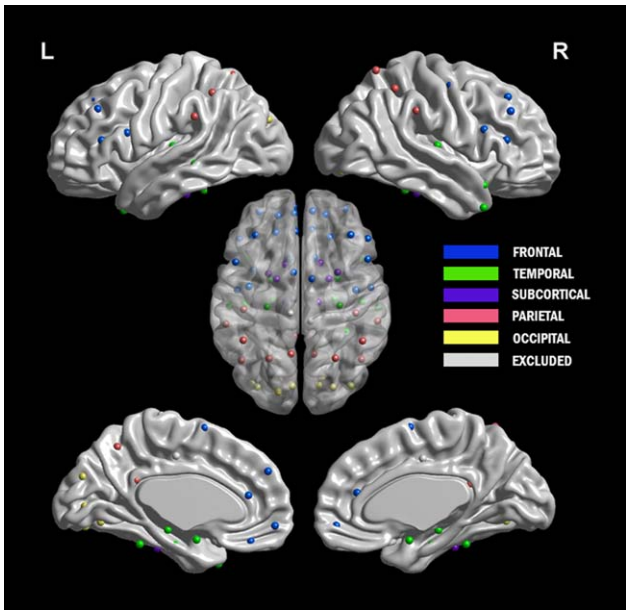

Figure 1.
The 90 brain regions used as seed locations and their corresponding regional groupings sorted by anatomical lobe, and arranged by colour. Blue = frontal, green = temporal, purple = subcortical, pink = parietal, yellow = occipital. Four regions were excluded from a lobar subgroup due to ambiguity in anatomical placement. Visualized with BrainNet Viewer [http://www.nitrc.org/projects/bnv, Xia et al. 2013].

Estimating functional connectivity using the weighted phase lag index

Functional interactions between sources of oscillatory activity can be captured by quantifying the phase relationship between their time series [see Pereda et al. 2005 for a review]. Although beamformer source reconstruction implements a spatial filter which aims to estimate the activity at the target location while attenuating contributions from other sources, beamformer reconstructed sources may still contain artificial and spurious interactions due to field spread and volume conduction. Artificial synchrony is directly caused by the instantaneous linear mixing of activity from nearby cortical areas and is removed using interaction metrics that detect exclusively lagged

interactions and suppress zero-lag synchrony. Spurious synchrony is detected in the area's neighboring sources [Palva and Palva, 2012] and can be suppressed by efficient cortical parcellation approaches [Palva et al. 2010]. In this study, we estimated functional connectivity using the recently introduced wPLI, which is an example of a mixing-insensitive interaction metric that attenuates artificial interactions [Vinck et al. 2011].

Briefly, the instantaneous phase at each time point of the filtered waveform was calculated for the 300-second recording using the Hilbert transform. WPLI was used to estimate phase synchrony between each source pair over 300 seconds of data, for each analyzed frequency range. For the mathematical definition of wPLI, see Vinck et al. [2011]. WPLI values range between zero (no phase locking) and one (total phase locking/synchronization), and are based on the magnitude of the imaginary component of the cross-spectrum. This limits the influence of cross-spectrum elements about the real axes, which are at risk of changing their "true" sign with small noise perturbations [Ortiz et al. 2012].[1] Similar to the PLI, the wPLI estimates to what extent the phase leads and lags between signals from two sources are nonequiprobable. In contrast to the PLI, however, wPLI gives maximal weighting to $\pm 90^{\circ}$ phase differences, and hence omits all signals associated with artificial synchrony [Lau et al. 2012]. Only phase lagging interactions, like those from a complex coupled oscillator system (i.e., synchronously oscillating neural assemblies), are detected. It has been shown that wPLI outperforms PLI, coherence, and imaginary coherence in attenuating volume conduction using real local field potential data [Vinck et al. 2011]. Moreover, wPLI has been demonstrated for measurement of inter-regional MEG synchrony in children [Dimitriadis et al. 2013], including graph analysis of resting-state connectivity [Ortiz et al. 2012].

Functional connectivity matrix construction

To describe brain networks a 90-by-90 connectivity matrix was computed for each subject for each frequency band. Group averages and group differences for each analyzed frequency range are presented in Figure 2. Connectivity matrices quantified the intensity of inter-regional functional connectivity between every pair of sources and were represented by the wPLI as described above. These connectivity matrices were used in subsequent lobar functional connectivity and NBS analyses described below.

[1]Various other methods have been employed for estimating inter-regional phase synchrony, including phase-locking values [Lachaux et al. 1999], the phase lag index [PLI, Stam et al. 2007] and nonlinear phase synchronization [Pereda et al. 2005]. Only interaction metrics that detect exclusively lagged interactions and suppress zero-phase lag synchrony, such as the imaginary coherence, imaginary part of the phase locking value, phase-slope index and the weighted phase-lag index are immune to artificial synchrony [Vinck et al. 2011].

Lobar functional connectivity and network-based statistic

We used two complementary approaches to describe pair-wise alterations in functional connectivity in ASD: (1) large-scale functional connectivity through lobar categorization of brain regions, which investigated resting synchrony within and between the lobes of the brain; (2) network-level functional connectivity analyzed using the NBS [Zalesky et al. 2010].

(1) To characterize neural synchrony within and between the lobes of the brain and to investigate alterations in connectivity expressed at the level of large-scale anatomical subdivisions of the brain, we sorted each source (region) based on lobar classification. There were five subgroups (subcortical structures and the four lobes) in accordance with the AAL atlas: frontal, temporal, subcortical, parietal, and occipital (Fig. 1), and similar to previous studies [Fornito et al. 2011; Hong et al. 2013]. Note that, hereafter, for the sake of brevity, we have generalized the term "lobe" to encompass the subgroup containing subcortical structures. Each subgroup contained between 8 and 32 nodes. Four regions [33, 34, 69, and 70] (Supporting Information Table S1) from the [90 × 90] connectivity matrices were removed due to ambiguity in anatomical placement into a lobe, and hence 86 of the 90 nodes were sorted. Connectivity within or between each lobar grouping was derived by averaging wPLI values across all edges (each pair of regions) relevant for that comparison. For example, theta band frontoparietal connectivity was obtained by averaging the wPLI values for each connection between a frontal source and a parietal source. We repeated this for each subject at each bandwidth, resulting in six [5 × 5] connectivity matrices per subject. To evaluate group differences in lobe-level functional connectivity, two-tailed t statistics were performed for each element of the [5 × 5] connectivity matrix in each frequency band. A false discovery rate (FDR) using a q-value of 0.05 was used to control for multiple comparisons [Benjamini and Hochberg, 1995].

(2) To describe in more detail which groups of regions were differentially connected in ASD adolescents, we employed the NBS [Zalesky et al. 2010]. This approach identifies networks—defined as contiguously connected sets of nodes—that are differentially connected between groups. An advantage of this approach over complex network analysis is that functional connectivity data can be readily related to anatomy; that is to say, clusters of regions that are functionally interconnected can be visualized in anatomical brain space.

In the NBS analysis, a primary threshold ($P = 0.0025$) was applied in a two-sample, one-tailed t-test for each edge in the [90 × 90] connectivity matrices to define a set of suprathreshold edges. This yielded a collection of contiguously connected components (groups of nodes) and their extent (number of significant connections/edges) was recorded. Then, to index the significance of each identified

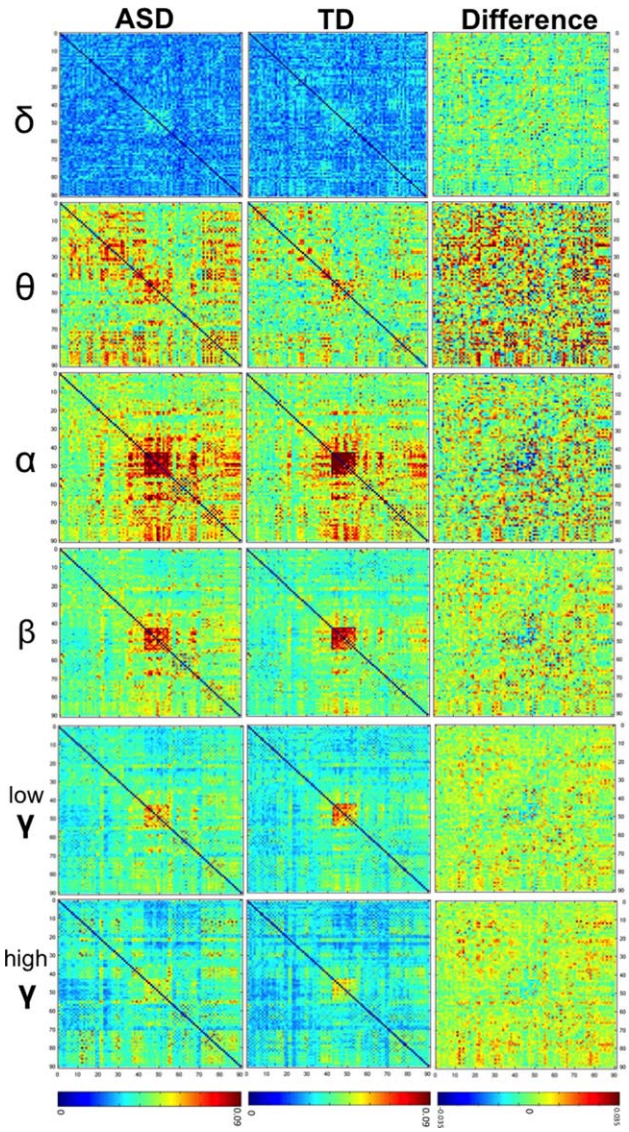

Figure 2.

Full connectivity matrices comprising 90 cortical and subcortical sources as defined by the Automated Anatomical Labeling atlas are shown for each of the six frequency bands and the two groups (columns labeled ASD and TD). The difference between the group average of ASD minus TD adolescents is also shown (column labeled Difference). Colour bar values depict wPLI values, or estimates of functional connectivity. The numbering of sources from 1–90 corresponds to Supporting Information Table S1.

component, a null distribution was empirically derived using nonparametric permutations (5,000 permutations). For each permutation, each subject was randomly reallocated into one of two groups, and differentially connected components in this surrogated data were identified using the same initial threshold that was applied to the unshuffled data ($P = 0.0025$). For a connected component of size M found for the real (nonshuffled) grouping of ASD participants and TD controls, a family-wise error corrected P-value was determined by calculating the proportion of the 5,000 permutations for which the maximal connected component was larger than M. Two alternative hypotheses (ASD adolescents > TD adolescents and TD adolescents > ASD adolescents) were evaluated independently for the six frequency bands. As the component extent of each value in the null distribution is obtained considering all pair-wise comparisons in the analyzed connectivity matrices, NBS controls for false positives due to multiple comparisons [Zalesky et al. 2010].

Global and local graph theory analyses

The wPLI results were used to construct a 90-by-90 weighted, undirected graph for each subject and analyzed frequency band, from which measures describing network topology were derived [see Bullmore and Sporns, 2009]. Detailed accounts of basic principles underlying graph analysis and its application to neuroimaging data have been published previously [Bullmore and Sporns, 2009; Rubinov and Sporns, 2010]. Given the past literature describing long-range hypoconnectivity and local hyperconnectivity in ASD, we were interested in measures pertinent to functional integration and segregation. To quantify this, we measured strength (overall connectivity), clustering coefficient (functional segregation) and path length (functional integration) of each subject's graph at each frequency band using the Brain Connectivity Toolbox [Rubinov and Sporns, 2010].

Specifically, path length is a measure of the shortest route (in terms of edges traversed) between two nodes [Rubinov and Sporns, 2010]. It is commonly referred to as a measure of functional integration [Rubinov and Sporns, 2010]. Average shortest path length, or characteristic path length, is the average shortest path length between all pairs of nodes in the network [Rubinov and Sporns, 2010]. Clustering coefficient, on the other hand, is a measure of functional segregation. The clustering coefficient is the likelihood that neighbours of a node are connected to each other, and indicates the extent of local interconnectivity or cliquishness in a network. For more details on graph theoretical measures see Bullmore and Bassett [2011] and Rubinov and Sporns [2010].

We quantified each graph measure for each individual node, as well as for the whole graph (obtained by averaging across all 90 analyzed nodes). For both the global and local graph analyses, a nonparametric permutation method with an alpha value set to 0.05 was adopted to evaluate statistical significance of group differences at each measure, for each frequency band. To provide surrogate data distributions, 2048 permutations were performed at an α-level of 0.05. This alpha level of 0.05 was then corrected via the t-max test [see Blair and Karniski, 1993] to account for multiple comparisons across all

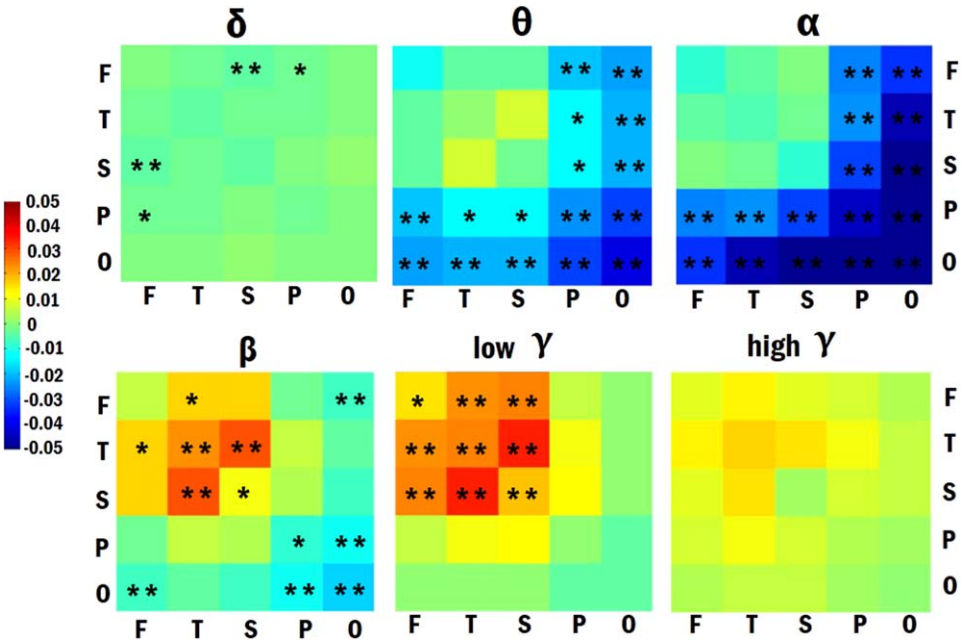

Figure 3.

Contrast of ASD and TD adolescents in group-averaged connectivity matrices for the six analyzed frequency bands. WPLI values depicted on the colour scale represent group differences (ASD minus TD) and were averaged by lobe grouping across both hemispheres. Uncorrected significant differences resulting from two-tailed *t* statistics are marked with one star (*$P < 0.05$ uncorrected), while FDR-corrected values are marked with two stars (**$P < 0.05$ FDR-corrected). F = Frontal, T = Temporal, S = Subcortical, P = Parietal, O = Occipital. Positive numbers (warm colours) represent increased connectivity in ASD; negative numbers (cool colours) reflect reduced connectivity in ASD.

network pairs and frequency bands. For local graph theory measures, to correct for the 90 independent tests (90 nodes in the graph), an alpha value of 1/90 ($P < 0.011$) was used as a threshold for statistical significance [Lynall et al. 2010].

RESULTS

Frequency- and Region-Dependent Alterations of Resting Synchrony in ASD

To facilitate characterization and interpretation of functional connectivity data from a large number of regions in the brain, we sorted connections represented in Figure 2 into regional clusters based on anatomical location (Fig. 1). This analysis approach enables the identification of alterations in resting synchrony which are expressed at levels of anatomical organization previously identified in the ASD literature (e.g. frontoparietal, frontofrontal, anterior–posterior). Group differences in within- and cross-lobar functional connections were statistically significant in five out of the six frequency bands ($P < 0.05$, FDR-corrected, Fig. 3). One of the primary observations from this large-scale, lobar analysis was a frequency- and region-specific pattern of overconnectivity and underconnectivity in the ASD group. In slower theta and alpha bands, occipital and parietal lobes expressed functional disconnection from widespread brain areas (including connections within these grouping themselves), with the most prominent effects observed in the alpha band. Conversely, faster gamma oscillations exhibited hyperconnectivity among frontal, temporal, and subcortical lobes in ASD adolescents. A more complex pattern of atypical intra- and interlobar connectivity was observed in the beta band, in which elements of the posterior disconnection were observed in concert with fronto-tempo-subcortical overconnection in the ASD group. Lastly, intralobar and interlobar connectivity in the delta band were similar between groups; however statistical differences between the two groups supported an anterior–posterior disconnection in the frontal cortex in ASD. No statistical differences in intralobe or interlobar functional connectivity were observed in the high gamma band.

For slow brain oscillations in the delta band, the parietal and subcortical lobes displayed significant decreases in functional connectivity with the frontal cortex ($P < 0.05$, uncorrected for frontoparietal, FDR-corrected for

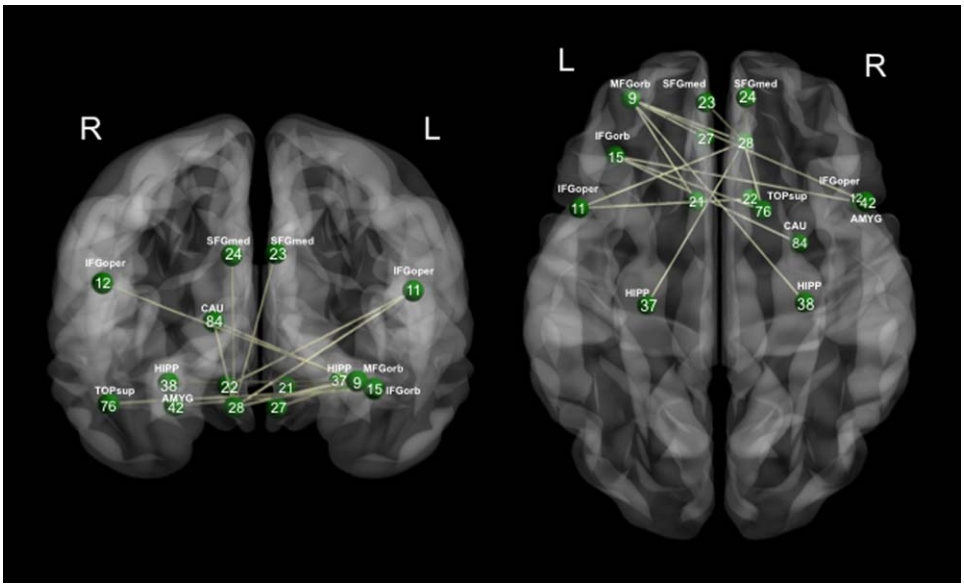

Figure 4.

Network consisting of 15 brain regions that were hyperconnected in ASD adolescents in the low gamma band. The connections (edges) between pairs of regions represent statistically significant differences in functional connectivity between the two groups. Network Based Statistic toolbox was used to compute statistics between strength of connections as indexed by wPLI values ($P = 0.012$ for the network). Landmark regions have been labelled with their respective abbreviated region names. For the full names and abbreviations of all regions, refer to Supporting Information Table I. Visualized with BrainNet Viewer [http://www.nitrc.org/projects/bnv, Xia et al. 2013].

frontosubcortical). Furthermore, intratemporal, intrasubcortical and intraparietal connections appeared hypoconnected in ASD. In the theta band, intralobar functional connectivity was lower in both parietal and occipital lobes and between these two lobes and the rest of the brain for the ASD group ($P < 0.05$, uncorrected for parietotemporal and parietosubcortical, FDR-corrected for all other connections). A more striking trend of functional disconnection in the same direction was found in the alpha band ($P < 0.05$, FDR-corrected). In the beta band, the ASD group had significantly higher functional temporotemporal, temporosubcortical, and subcorticosubcortical connectivity ($P < 0.05$, FDR-corrected). In contrast, frontooccipital, parietooccipital, and occipitooccipital beta band connections were lower in ASD adolescents compared to TD adolescents ($P < 0.05$, FDR-corrected). In the low gamma band, all intra- and interlobar connections between the frontal, temporal, and subcortical lobes were significantly higher in the ASD group ($P < 0.05$, uncorrected for frontofrontal connections, FDR-corrected for all other connections). Finally, despite lack of statistical differences between groups in the high gamma band, the temporal lobes appeared overconnected to the frontal cortex, to subcortical regions and to themselves.

Increased Gamma-Band Network Synchrony in ASD

NBS is a method to detect functionally interconnected (functionally integrated) nodes in a graph that cluster into a single component, and which are significantly different between two groups. In our study, NBS analysis revealed a single significant network ($P = 0.012$, see Fig. 4 for details). This network consisted of 15 nodes that were overconnected in the ASD group, in the low gamma band, consisting of frontal, temporal, and subcortical regions. Each region has been indexed by its region number, corresponding to Table S1 in the Supporting Information. Of note, the region with the greatest number of significantly different connections was the orbital part of the left middle frontal gyrus (MFGorb). Specifically, the left MFGorb was hyperconnected to the left and right rectal gyri, the opercular part of the right inferior frontal gyrus (IFG), the right hippocampus, and the left olfactory cortex. These NBS results are congruent with the large-scale lobar connectivity findings noted above for the low gamma band, and indicate a specific network of hyperconnected nodes anchored in prefrontal cortex. No significantly connected components in the other five frequency bands were observed using the NBS approach.

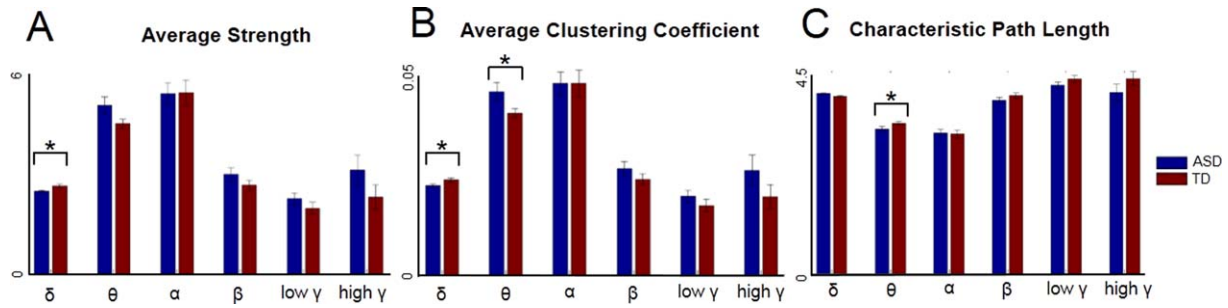

Figure 5.

Differences in measures of global topological attributes of brain connectivity between ASD and TD adolescents derived from global graph theoretical analysis. Significant differences (marked with one star) were found between the two groups for delta and theta frequency bands ($P < 0.05$, FDR-corrected). **A**, Average strength of the whole network comprising 90 nodes for each frequency range. **B**, Average clustering coefficient of the whole network for each frequency range. **C**, Characteristic path length of the whole network for each frequency range. Blue = ASD, red = TD adolescents. [Color figure can be viewed in the online issue, which is available at wileyonlinelibrary.com.]

Frequency-Dependent Alterations in Global Network Topology in ASD

To investigate the hypothesis that network topology of spontaneous MEG activity is altered in adolescents with ASD, graph analyses were applied at the global (whole graph) and local (each node) levels to each subject's graph of resting phase synchrony for each of the six analyzed frequency bands. At the global level, we compared average strength, average clustering coefficient, and characteristic path length of the two groups. Figure 5 depicts group averages for each global measure for each frequency band. Significant differences between the groups were observed for low-frequency oscillations (delta and theta) but not in the higher-frequency bands ($P < 0.05$, FDR-corrected).

Similar to our results from investigation of large-scale anatomical organization within and between the lobes of the brain, alterations in network topology in ASD were also expressed in a frequency-dependent manner. Overall, we found a general trend for increased "local connectedness"—increased global clustering coefficient coupled with decreased path length—of the functional network (theta, beta, low, and high gamma bands). By contrast, networks in the alpha frequency range were similar between groups, while delta band alterations in network topology showed effects in the opposite direction. Taken together, results at the 'whole network' level suggest alterations in functional integration and segregation of regional clusters in adolescents with ASD. Of note, average clustering coefficient in delta and theta bands were significantly different between the groups ($P < 0.05$, FDR-corrected), whereas characteristic path length was only significantly different in theta band ($P < 0.05$, FDR-corrected). Average strength differences between groups were significant in the delta frequency range, where higher resting synchrony was observed in the TD adolescents ($P < 0.05$, FDR-corrected).

Atypical Regional Topologies in Adolescents with ASD

Network topology was also investigated at each of the 90 nodes in order to capture alterations in brain network organization pertaining to the connectedness of particular brain regions in ASD. This analysis revealed significant between-group differences in nodal strength, nodal clustering coefficient, and nodal path length in five of the six analyzed frequency ranges ($P < 0.011$ corrected, Table I). Congruent with our findings using global network measures, nodal-level measures "local connectedness" (clustering coefficient and path length) were higher in theta, beta, low, and high gamma band in ASD, but were decreased in the delta band, with no differences present in the alpha band. Overall, adolescents with ASD exhibited disrupted local segregation and integration of functional networks compared to TD adolescents. There were 13 nodes (regions) which were significantly different in local graph properties between the two groups; close to half of the regions belonged to the frontal lobes, including orbital and medial orbital parts of the superior frontal gyrus, the gyrus rectus, the orbital part of the middle frontal gyrus, and the pars triangularis of the inferior frontal gyrus ($P < 0.011$ corrected, Table I).

DISCUSSION

This study provides the first source-resolved investigation of resting-state oscillatory synchrony in ASD. We provide new insights into the role of specific networks and

TABLE I. Group comparisons (ASD adolescents minus TD adolescents) of complex network measures characterizing functional segregation and integration using local graph theory analysis

Frequency band	Region number	Region name	Difference (ASD minus TD)	*P* value	Lobe
(A) Nodal strength					
Δ	6	R.SFGorb	−0.42	0.008	Frontal
	61	L.IPL	−0.33	0.010	Parietal
	62	R.IPL	−0.32	0.009	Parietal
Θ	14	R.IFGtri	1.2	0.003	Frontal
	67	L.PCUN	1.0	0.008	Parietal
B	46	R.CUN	−0.48	0.009	Occipital
	56	R.FUSI	0.85	0.004	Temporal
Low γ	9	L.MFGorb	0.54	0.004	Frontal
	28	R.REC	0.94	0.0005	Frontal
High γ	73	L.STG	2.1	0.004	Temporal
	77	L.MTG	2.1	0.009	Temporal
(B) Nodal clustering coefficient					
Δ	6	R.SFGorb	−3.1	0.004	Frontal
	25	L.SFGmorb	−2.8	0.006	Frontal
	28	R.REC	−3.2	0.009	Frontal
	60	R.SPG	−2.4	0.010	Parietal
	61	L.IPL	−2.4	0.008	Parietal
	77	L.MTG	−4.3	0.010	Temporal
Θ	14	R.IFGtri	9.5	0.0010	Frontal
	61	L.IPL	5.0	0.008	Parietal
	67	L.PCUN	8.5	0.004	Parietal
Low γ	28	R.REC	6.4	0.0010	Frontal
(C) Nodal path length					
Δ	61	L.IPL	1.6	0.006	Parietal
Θ	14	R.IFGtri	−3.0	0.002	Frontal
B	46	R.CUN	2.1	0.008	Occipital
	56	R.FUSI	−3.2	0.007	Temporal
Low γ	9	L.MFGorb	−3.5	0.0005	Frontal
	28	R.REC	−4.5	0.0005	Frontal

Nodes that were significantly different between the groups are denoted by their region number and abbreviated region name, corresponding to Supporting Information Table I, and sorted by frequency band. Corresponding *P*-values for group differences are also listed, in addition to the lobar subgrouping of each node. A negative difference in nodal graph metrics represents ASD < TD adolescents, whereas a positive difference in graph metrics represents ASD > TD adolescents. A, Nodal strength differences. B, Nodal clustering coefficient differences. C, Nodal path length difference. To determine significance, an alpha value of 1/90 or $P < 0.011$ was used. Note that no group differences in the alpha frequency range were detected for local graph theory analysis.

brain regions which exhibit altered neurophysiological interactions in this population. Our findings indicate that adolescents with ASD demonstrate atypical neural oscillatory synchrony in a region- and frequency band-dependent manner. Specifically, occipital and parietal brain regions were found to express low frequency functional disconnection from widespread brain regions in adolescents with ASD, whereas overconnectivity at higher frequencies was observed among frontal, temporal, and subcortical areas. We also found a hyperconnected subnetwork in the low gamma frequency range, which included many regions of frontal cortex, as well as left and right hippocampi, right amygdala, right caudate nucleus, and right superior temporal gyrus (STG). Moreover, ASD adolescents expressed atypical network topologies at both global and local levels, indicating abnormal functional integration and segregation in large-scale brain networks. Together, our study provides empirical evidence for the disruption of topological organization of functional networks in ASD.

Altered EEG and MEG Resting Connectivity in ASD

Functional disconnection of the parietal and occipital cortices from other cortical regions at lower frequencies (delta, theta, and alpha) was observed in ASD adolescents, in which the alpha band was the most striking. Decreased alpha coherence has been previously reported at the

sensor/electrode level in resting-state EEG studies in children [Coben et al. 2008] as well as adults with ASD [Murias et al. 2007]. We did not, however, observe a significant frontal [Murias et al. 2007] or temporal [Coben et al. 2008] disconnection from the rest of the cortex in theta or alpha bands albeit nonsignificant decreases in interlobar connectivity of frontal and temporal lobes in ASD in comparison to TD were noted. Although frontal and temporal connections to the occipital and parietal lobes were significantly hypoconnected in the present study, effects appeared to be driven by the low-frequency disengagement of posterior regions from widespread brain areas. In delta and theta bands, lower coherence in ASD has been reported previously in parietal and occipital regions [Coben et al. 2008], in addition to temporal and central regions which we did not observe.

Interestingly, our results contrast those from a recent resting-state MEG study that reported increased long-range connectivity in the temporal, parietal, and occipital lobes in alpha band [Ghanbari et al. 2013]. The differences between this study and ours could be attributed to factors such as differences in age groups (children and adults versus adolescents), eye state (closed versus open), analysis level (sensor-space versus source-space), parcellation scheme (sensor-groups versus atlas-based seeds) and functional connectivity metric (synchronization likelihood versus wPLI). Moreover, the results presented here are likely to be more accurate with respect to specific brain regions and networks involved in altered oscillatory synchrony in ASD, as analysis of EEG/MEG connectivity among reconstructed sources is substantially more accurate than sensor-based approaches in this regard [Schoffelen and Gross, 2009].

ASD Adolescents Express Decreased Anterior-Posterior Connections at Slow Frequencies

Deficient long-range connections along anterior–posterior brain pathways could disrupt experience-dependent processes during development that are important for creating and maintaining neural connections [see Geschwind and Levitt, 2007 for review]. Atypical maturation of connectivity could hinder the development of social cognitive abilities such as joint attention and social responsiveness, which reliably discriminate young children with ASD from their TD peers [Baranek, 1999; Werner et al. 2000; Wetherby et al. 2004]. Evidence of reduced coherence between anterior and posterior brain regions on the basis of resting EEG data [Coben et al. 2008; Murias et al. 2007] supports this hypothesis. The view that frontoposterior connectivity is reduced in ASD is also supported by several lines of evidence from structural and functional MRI studies [see Just et al. 2012 for review]. Our findings using source-space analysis of resting neurophysiological synchrony in adolescents with ASD are congruent with the above hypothesis at low frequency oscillations below 30 Hz. However, our results also suggest an extension to the disconnection theory: (1) that aberrant features of brain organization are expressed in a frequency-dependent manner; and (2) both cortical and subcortical systems are affected.

The Hyperconnected Gamma Subnetwork May Reflect Socioemotional Deficits in ASD

Gamma oscillations are regarded as important as they are believed to coordinate precise synchronization in local circuits, and accordingly, play a vital role in information processing supporting cognition [Fries, 2009]. Converging evidence suggests that properties of gamma oscillations are altered in ASD during task performance [Orekhova et al. 2007; Rojas et al. 2011; Stroganova et al. 2012; Wilson et al. 2007]. Our finding of increased connectivity in the ASD group in a subnetwork of medial frontal, temporal and subcortical regions is of twofold interest; it lends support to the view that altered gamma-oscillatory processes play a role in the pathophysiology of ASD, and demonstrates that, in particular, affected regions in this subnetwork include regions understood to be critical for social cognition.

The theory that excess high frequency oscillations reflect an imbalance in the excitation-inhibition homeostasis in the cortex [Orekhova et al. 2007] may be relevant to findings of gamma-band hyperconnectivity in ASD. Mutations in genes involved in the expression of excitatory and inhibitory neurotransmitters have been identified in ASD populations [Collins et al. 2006; Ramoz et al. 2004] as well as animal models of ASD [DeLorey et al. 2008]. This may provide the basis for a link between atypical oscillations and genetic mechanisms underlying ASD, as individual differences in the expression of gamma oscillations have been demonstrated to be under tight genetic control [van Pelt et al. 2012].

With respect to social cognition, there are several regions within the significantly different, hyperconnected gamma band subnetwork in ASD (identified using NBS) that are of particular interest. Such hyperconnected regions include the IFG and regions encompassing the "social brain": the orbitofrontal areas, the amygdalae, the STG [Brothers, 1990], and the medial frontal cortex [Amodio and Frith, 2006]. Hyperconnectivity amongst regions critical for social cognition, in concert with hyperconnectivity to other regions of a different functional network may disrupt task-relevant communication among brain regions underlying social cognitive abilities [Lynch et al. 2013]. Alternatively stated, atypical connectivity among these regions may limit dynamic interactions amongst the rest of the cortex [Uddin et al. 2013].

One region of particular interest is the IFG due to its role in language, social cognition, and emotion processing. The IFG is vital for speech and language processing, as it is responsible for both semantic and syntactic processing

of linguistic inputs, in addition to the motor production of speech [Bookheimer, 2002]. The mirror neuron system, located in the IFG, is a neural mechanism by which others' actions and intentions can be understood [see Rizzolatti and Craighero, 2004 for review], and its dysfunction was proposed to give rise to the cascade of impairments that are characteristic of ASD [see Williams et al. 2001 for review]. In addition, atypical activation in fMRI has been demonstrated in the IFG during emotion processing tasks [Fusar-Poli et al. 2009; Kesler-West et al. 1999], suggesting aberrant connectivity of this region in ASD populations.

Another key observation from the NBS analysis relates to the functional role of two limbic regions: the right amygdala and the hippocampi. Converging evidence from studies in human and animals suggests that emotion perception and regulation is mediated by a brain circuit in which the amygdalae and hippocampi are central components. The amygdalae play a key role in the recognition and evaluation of emotionally salient stimuli and subsequent production of affective states [Phillips et al. 2003]. The right amygdala in particular, is linked to implicit emotional processing [Adolphs et al. 2005; Costafreda et al. 2008; Hung et al. 2012; Noesselt et al. 2005]. The hippocampi, apart from their general role in memory, modulate the production of contextually appropriate affective behavior that is elicited by emotionally salient stimuli. The hippocampi do this through inhibitory connections with the amygdalae and other structures involved in emotion perception [Phillips et al. 2003]. Interestingly, in childhood, several studies have supported the idea of enlarged amygdalae and hippocampi in ASD [Groen et al. 2010; Howard et al. 2000; Rojas et al. 2006; Schumann et al. 2004; Sparks et al. 2002], with volume losses that emerge in adulthood [Duerden et al. 2012; Nickl-Jockschat et al. 2012; Yu et al. 2011]. Our findings of hyperconnectivity in the left and right hippocampi along with the right amygdala support the idea of a developmental abnormality in these regions in ASD, which persists into adolescence.

The last region of particular interest to highlight from the hyperconnected low gamma subnetwork revealed by NBS is the caudate nucleus. This nucleus thought to be part of an intricate system integrating multimodal information and regulating complex behavior [Alexander and Crutcher, 1990; Haber, 2003]. The caudate is also increasingly recognized to be implicated in affect processing [Arsalidou et al., 2013]. Given these associations, hyperconnectivity of the caudate nucleus in the current study could be associated with corticostriatal feedback and may therefore be related to behavioral problems in ASD. In line with this, stereotypic, repetitive behavior patterns related to the diagnostic criteria for ASD have been compared to those seen in obsessive-compulsive disorders, which are known to be associated with structural and functional abnormalities in the basal ganglia [Langen et al. 2009]. Furthermore, in a voxel-based morphometry longitudinal study characterizing the developmental trajectories of striatum in ASD, an increase was detected in caudate volumes in ASD, while it decreased in control subjects [Langen et al. 2009]. Taken together, our findings regarding the overconnected subnetwork in the low gamma frequency band can be interpreted considering the postulate that daily life, with its social demands and constantly changing situations, imposes additional social cognitive demands in adolescents with ASD resulting in abnormal information processing in regions related to social cognition, behavior, and emotion perception and regulation.

Differences in Global Network Topology Indicated Disrupted Functional Integration and Segregation in ASD

At the 'whole network' level, our results indicated ASD adolescents exhibited disrupted functional integration and segregation of brain networks. In particular, we demonstrated differences in average strength, clustering coefficient and characteristic path length at both low and high frequencies, suggesting a less optimized topological organization in functional networks of adolescents with ASD. Furthermore, increased average clustering coefficient and shorter characteristic path length in theta, beta, low and high gamma bands indicate increased "cliquishness" properties of functional networks within these frequency ranges, supporting the idea of disrupted balance between global integration and local specialization. On the network level, this suggests a pattern of global overconnectivity and altered network topology favouring increased clusters of local connections in ASD. Moreover, stronger local connectivity has been previously reported in structural studies of autism using diffusion tensor imaging [Herbert et al., 2004; Li et al 2014].

It is possible that the overabundance of short functional connections could be related to redundant connectivity patterns and to proposed neurobiological mechanisms in ASD. In normal early development, overconnectivity is followed by a pruning of connections in the maturing brain [Supekar et al. 2009], suggesting network refinement [Hagmann et al. 2010]. Physiologically, in ASD, impaired pruning of connections in this dynamic process would result in the redundancy of connections. Hence, the remaining overconnected network may operate at different scales, resulting in a poor signal-to-noise ratio where the system is flooded with noise in the event of an incoming signal [Belmonte et al., 2004]. With poor signal-to-noise ratio, the output of the functional network may not be sufficiently distinct (too much integration and not enough segregation) to achieve the necessary information processing [Rippon et al. 2007]. In addition, recent work has demonstrated that brain maturation is reflected in a weakening of short-range and a strengthening of long-range connectivity [Dosenbach et al. 2010]. From this perspective, our findings may reflect a more immature connectivity pattern in adolescents with ASD.

There are some interesting nuances to this trend in globally altered network topologies that deserve mention. First, delta band measures of global network topology exhibit the opposite pattern of effects in ASD: networks have decreased average strength, decreased clustering coefficient and increased characteristic path length. This suggests a loss of functional segregation of networks in ASD. In the model of autism as a developmental disconnection syndrome, decreased functional segregation could be anticipated as it suggests that specific functional systems are less distinct or functionally segregated from one another. Second, although there is a general trend for global overconnectivity in ASD, alpha band functional networks appear to be relatively the same between the two groups. As average strength is a direct reflection of mean coherence (functional connectivity) within the network, our results suggest that there is no significant overall difference in phase synchrony at rest in alpha bands in adolescents with ASD compared to controls. This result is not surprising as it has been previously reported in resting EEG studies in ASD [Mathewson et al. 2012; Peters et al. 2013].

Focal Disruptions in ASD Involve the Default Mode Network, Frontal Cortex and the Temporoparietal Junction

When we looked at local graph measures to describe focal alterations in specific regions of the brain, we found three observations of interest in the ASD literature. First, several regions that displayed significant alterations in focal topology were implicated in the default mode network (DMN), such as the precuneus and the inferior parietal lobule. Second, five of the thirteen nodes that were significantly different in local graph properties in ASD belonged to the frontal cortex. Lastly, in the high gamma band, focal alterations were detected in theory of mind (ToM)-relevant regions in the ASD group. One of the primary observations from the regional graph analysis relates to alterations in regions encompassing the DMN. The delta band group differences provide a particularly salient example of these alterations involving DMN regions. Decreased nodal strength, decreased clustering coefficient and increased path length in nodes of the DMN in delta band suggest loss of functional segregation within this network. In contrast, theta and high gamma bands reveal the opposite direction of effects in DMN regions; such regions appeared to be hyperconnected and demonstrate increased local functional connectedness. We propose that these findings—though seemingly opposite in effect—both suggest that regions involved in the DMN are functionally disrupted. In other words, adolescents with ASD may exhibit a less optimized topological organization in the DMN, leading to frequency-dependent functional alterations in DMN regions. Accordingly, decreased clustering coefficient may relate to decreased functional segregation (i.e., delta band findings) of the DMN to the rest of the brain, while increased clustering coefficient may suggest lack functional specialization (i.e., theta, beta, low gamma band findings) due to an abundance of functional connections. Interestingly, evidence from structural and fMRI in ASD have reported both underconnectivity [Assaf et al. 2010; Stigler et al. 2011] and overconnectivity [Lynch et al. 2013; Uddin et al. 2013; Redcay et al. 2013] between DMN nodes.

The frontal lobes are responsible for numerous higher-order cognitive functions, including planning, decision making and abstraction, and thus are a primary candidate for dysfunction in many neurodevelopmental and neuropsychiatric disorders. We report 5 out of 13 altered focal topologies in the frontal cortex, suggesting a less organized or more random distribution of functional networks involving frontal areas. Although our findings revealed altered local functional connectivity in the frontal lobes, we are limited in terms of the conclusions we can make regarding the anatomical proximity of these functional hyperconnections. In light of our large-scale lobar connectivity results, it is plausible that short-range connections involving the frontal cortex are underconnected at lower frequencies (e.g., delta band) and overconnected at higher frequencies (e.g., low gamma band). Even though current theory purports that there is local overconnectivity in the frontal cortex in ASD [Courchesne and Pierce, 2005], literature from multiple modalities involving task-based and task-free paradigms have been inconclusive in supporting this hypothesis [see Vissers et al. 2012, for review]. Nonetheless, the abnormal functional properties of frontal regions are interesting in light of both the association between ASD and the current frontal hyperconnectivity theory and evidence of frontal involvement in the DMN.

Another inference that may be drawn from observations from local graph theory results relates to regions implicated in ToM. The impairment of ToM (processing of mental states of others) in ASD has been linked to difficulties with the communications and interactions in everyday life [Kana et al. 2009]. The temporoparietal junction (TPJ), in particular, is thought to be central to the integration of social information and empathy, in addition to selective attention to salient stimuli (Decety and Lamm, 2007]. In the high gamma band, two regions surrounding the TPJ demonstrated altered focal topology in our study: the left superior and medial temporal gyri. In children, adolescents and adults with ASD, thinning of several regions in the TPJ region, particularly on the left side, has been reported [Greimel et al. 2013; McAlonan et al. 2005; Raznahan et al. 2010; Wallace et al. 2010]. Although our findings of increased local strength in TPJ regions are not immediately intuitive when considering neurological reports of volume reductions, it is suggestive of altered function within these regions that could interfere with ToM-related information processing.

In general, we found alterations in global and local graph analyses supporting increased local connectedness

in functional brain networks in ASD. We propose that increased local connectedness could imply decreased functional specialization of brain regions in ASD. Connections in the brain are formed at a high physical cost [Bullmore and Sporns, 2009; Sporns and Zwi, 2004] and the brain constantly negotiates the trade off between wiring costs and topological efficiency [Bullmore and Sporns, 2012]. Our findings of increased average strength in ASD and increased local connectedness suggest impaired network refinement in this population, particularly at a critical time of development in adolescence.

Limitations and Future Work

Some important caveats should be considered with regard to the present study. First, the limits of MEG in localizing and estimating the activity of deep brain sources remain an area of on ongoing research. Multiple studies have shown MEG to be effective at detecting weak signals emanating from deep brain structures such as the hippocampi during a variety of tasks [Cornwell et al. 2008a; Ioannides et al. 1995; Kirsch et al 2003; Nishitani et al. 1998], as well as the amygdala [Cornwell et al. 2007, 2008b, 2010; Hung et al. 2010; Ioannides et al. 1995; Liu et al. 1999; Luo et al. 2007; Moses et al. 2007; Streit et al. 1999] and thamalus [Bardouille and Ross, 2008; Bish et al. 2004; Tesche, 1996]. Moreover, there have been several realistic simulations that have shed light on parameters affecting our ability to detect such sources of activity [Balderston et al. 2014; Mills et al. 2012; Quraan et al. 2011]. Despite this empirical evidence, the debate over the ability of MEG to accurately detect and localize deep sources has persisted [for in-depth discussion see Riggs et al. 2009; Stephen et al. 2005]. With this in mind, our findings regarding connectivity alterations involving deep brain sources in this study should be interpreted with a degree of caution.

Another issue is the effect of sorting brain regions into their anatomical, lobar subdivisions. Since each lobe is different in size, numbers of regions/nodes sorted into each were accordingly different. This results in an uneven number of regions for each lobe, so it is plausible that a small number of connections within a lobe may have exerted a disproportionate influence on the resulting depiction of lobar connectivity. To address this issue, we describe regional differences between the two groups using bivariate statistics (NBS) in addition to both global and nodal graph theory measures, which do not suffer from this limitation. We feel this level of description is nonetheless informative given prior theory and experimental reports describing altered connectivity in ASD at the level of large-scale anatomical systems.

Third, while the atlas-based whole brain reconstruction of MEG source activity has been shown to be a valuable approach for investigating connectivity in large-scale brain networks, there are some limitations when using this method. For instance, the selection of sources is sparse and may not yield an accurate or adequate selection of brain structures that contribute to a more complete understanding of the brain in ASD. Such limitations might be ameliorated by adopting a whole-brain parcellation scheme that is based on source sensor geometry to obtain a set of maximally independent patches [Palva et al 2010]. While such advances are excellent in addressing some experimental questions in normative studies, however, they introduce additional complications for our experimental question related to ASD. Specifically, it has been established that there are reliable structural brain differences in ASD, and as such, parcellation approaches which use structural information to define cortical "patches" for analyses may introduce potential confounds to the study (i.e., systematic group differences in brain morphology may introduce systematic differences in patch location, complicating interpretation of the results). Nonetheless, we feel the disadvantages of using a standard brain-atlas are outweighed by the important advantage that it enables a more direct comparison between data from different modalities, especially in the context of heterogeneity in ASD findings.

Recently, there has been an emergence of evidence indicating brain overconnectivity in children with autism, contrasting multiple prior reports of underconnectivity in ASD [Di Martino et al. 2014; Keown et al. 2013; Supekar et al. 2013; Uddin et al. 2013]. These studies in resting-state fMRI report hyperconnectivity in both long- and short-range intrinsic connections across multiple brain regions in young children with ASD. Such findings add weight to the argument that hyperconnectivity outweighs hypoconnectivity in ASD, while also painting a more complicated picture regarding where disrupted brain connectivity in ASD may be dependent on altered age-related trajectories. In view of these recent findings, a limitation to our study is the lack of longitudinal data in our cohort of ASD participants to comprehensively address this question. Furthermore, as adolescence is a period of heavy grey matter development within the brain, it will be interesting to characterize whether the functional alterations reported are directly related to structural alterations due to a difference in developmental trajectory in this population. Future research should elucidate the developmental trajectory of altered MEG connectivity in ASD, as well at the relations between atypical neurophysiological interactions and underlying brain structure.

CONCLUSIONS

The results of the present study provide the first evidence of frequency- and region-specific alterations of resting-state neurophysiological interactions in ASD. These results provide valuable complementary evidence to the growing literature indicating that ASD is associated with atypical brain connectivity. We demonstrate that frontal

overconnectivity is expressed in the gamma band, whereas posterior brain regions exhibit a disconnection to widespread brain areas in slower delta, theta and alpha bands. Frequency-dependent alterations in network topology were also detected at both global and local levels of functional networks, suggesting an imbalance in cortical segregation and integration in functional brain networks. Moreover, we uniquely demonstrate atypical high-frequency network topologies involving frontal regions that are critical for social cognition, affording new insights into relations between neural oscillations, brain connectivity and social cognitive deficits in ASD.

ACKNOWLEDGMENTS

The authors thank the children and families who participated; Marc Lalancette, Tammy Rayner, and Ruth Weiss for their help in data collection; Tamara Powell and Vanessa Vogan for their help with recruitment and assessment of participants; Ryan Anderson and Simeon Wong for their technical help in construction of the data analysis pipeline; and George Ibrahim, Wayne Lee, and Benjamin R. Morgan for many stimulating discussions.

REFERENCES

Adolphs R, Gosselin F, Buchanan TW, Tranel D, Schyns P, Damasio AR (2005): A mechanism for impaired fear recognition after amygdala damage. Nature 433:68–72.

Alexander GE, Crutcher MD (1990): Functional architecture of basal ganglia circuits: Neural substrates of parallel processing. Trends Neurosci 13:266–271.

American Psychiatric Association. (2013): Diagnostic and statistical manual of mental disorders, 5th ed. Arlington, VA: American Psychiatric Publishing.

Amodio DM, Frith CD (2006): Meeting of minds: The medial frontal cortex and social cognition. Nat Rev Neurosci 7:268–277.

Arsalidou M, Duerden EG, Taylor MJ (2013): The centre of the brain: Topographical model of motor, cognitive, affective, and somatosensory functions of the basal ganglia. Hum Brain Mapp 34:3031–3054.

Assaf M, Jagannathan K, Calhoun VD, Miller L, Stevens MC, Sahl R, O'Boyle JG, Schultz RT, Pearlson GD (2010): Abnormal functional connectivity of default mode sub-networks in autism spectrum disorder patients. Neuroimage 53:247–256.

Balderston NL, Schultz DH, Baillet S, Helmstetter FJ (2014): Rapid amygdala responses during trace fear conditioning without awareness. PLoS One 9:e96803.

Baranek GT (1999): Autism during infancy: A retrospective video analysis of sensory-motor and social behaviors at 9–12 months of age. J Autism Dev Disord 29:213–224.

Bardouille T, Ross B (2008): MEG imaging of sensorimotor areas using inter-trial coherence in vibrotactile steady-state responses. Neuroimage 42:323–331.

Belmonte MK, Allen G, Beckel-Mitchener A, Boulanger LM, Carper RA, Webb SJ (2004): Autism and abnormal development of brain connectivity. J Neurosci 24:9228–9231.

Benjamini Y, Hochberg Y (1995): Controlling the false discovery rate—A practical and powerful approach to multiple testing. J R Statist Soc Series B 57:289–300.

Bish JP, Martin T, Houck J, Ilmoniemi RJ, Tesche C (2004): Phase shift detection in thalamocortical oscillations using magnetoencephalography in humans. Neurosci Lett 362:48–52.

Blair RC, Karniski W (1993): An alternative method for significance testing of waveform difference potentials. Psychophysiology 30:518–524.

Bookheimer S (2002): Functional MRI of language: New approaches to understanding the cortical organization of semantic processing. Annu Rev Neurosci 25:151–188.

Brothers L (1990). The social brain: A project for integrating primate behavior and neurophysiology in a new domain. Concepts Neurosci. 1:27–51.

Bullmore E, Sporns O (2009): Complex brain networks: Graph theoretical analysis of structural and functional systems. Nat Rev Neurosci 10:186–198.

Bullmore ET, Bassett DS (2011): Brain graphs: Graphical models of the human brain connectome. Annu Rev Clin Psychol 7:113–140.

Bullmore E, Sporns O (2012): The economy of brain network organization. Nat Rev Neurosci 13:336–349.

Cheyne D, Bakhtazad L, Gaetz W (2006): Spatiotemporal mapping of cortical activity accompanying voluntary movements using an event-related beamforming approach. Hum Brain Mapp 27: 213–229.

Cheyne D, Bostan AC, Gaetz W, Pang EW (2007): Event-related beamforming: A robust method for presurgical functional mapping using MEG. Clin Neurophysiol 118:1691–1704.

Coben R, Clarke AR, Hudspeth W, Barry RJ (2008): EEG power and coherence in autistic spectrum disorder. Clin Neurophysiol 119:1002–1009.

Cornwell BR, Baas JM, Johnson L, Holroyd T, Carver FW, Lissek S, Grillon C (2007): Neural responses to auditory stimulus deviance under threat of electric shock revealed by spatially-filtered magnetoencephalography. Neuroimage 37:282–289.

Cornwell BR, Johnson LL, Holroyd T, Carver FW, Grillon C (2008a): Human hippocampal and parahippocampal theta during goal-directed spatial navigation predicts performance on a virtual Morris water maze. J Neurosci 28:5983–5990.

Cornwell BR, Carver FW, Coppola R, Johnson L, Alvarez R, Grillon C (2008b): Evoked amygdala responses to negative faces revealed by adaptive MEG beamformers. Brain Res 1244: 103–112.

Cornwell BR, Salvadore G, Colon-Rosario V, Latov DR, Holroyd T, Carver FW, Coppola R, Manji HK, Zarate CA, Jr., Grillon C (2010): Abnormal hippocampal functioning and impaired spatial navigation in depressed individuals: evidence from whole-head magnetoencephalography. Am J Psychiatry 167:836–844.

Cornew L, Roberts TPL, Blaskey L, Edgar JC (2012): Resting-state oscillatory activity in autism spectrum disorders. J Autism Dev Disord 42:1884–1894.

Costafreda SG, Brammer MJ, David AS, Fu CH (2008): Predictors of amygdala activation during the processing of emotional stimuli: A meta-analysis of 385 PET and fMRI studies. Brain Res Rev 58:57–70.

Courchesne E, Pierce K (2005): Brain overgrowth in autism during a critical time in development: Implications for frontal pyramidal neuron and interneuron development and connectivity. Int J Dev Neurosci 23:153–170.

Decety J, Lamm C (2007): The role of the right temporoparietal junction in social interaction: How low-level computational processes contribute to meta-cognition. Neuroscientist 13:580–593.

DeLorey TM, Sahbaie P, Hashemi E, Homanics GE, Clark JD (2008): Gabrb3 gene deficient mice exhibit impaired social and exploratory behaviors, deficits in non-selective attention and hypoplasia of cerebellar vermal lobules: A potential model of autism spectrum disorder. Behav Brain Res 187:207–220.

Diaconescu AO, Alain C, McIntosh AR (2011): The co-occurrence of multisensory facilitation and cross-modal conflict in the human brain. J Neurophysiol 106:2896–2909.

Dichter GS (2012): Functional magnetic resonance imaging of autism spectrum disorders. Dialogues clin neurosci 14:319–351.

Di Martino A, Yan CG, Li Q, Denio E, Castellanos FX, Alaerts K, Anderson JS, Assaf M, Bookheimer SY, Dapretto M and others (2014): The autism brain imaging data exchange: towards a large-scale evaluation of the intrinsic brain architecture in autism. Mol Psychiatry 19:659–667.

Dimitriadis S, Laskaris N, Simos P, Micheloyannis S, Fletcher J, Rezaie R, Papanicolaou A (2013): Altered temporal correlations in resting-state connectivity fluctuations in children with reading difficulties detected via MEG. Neuroimage.83:307–317.

Dosenbach NU, Nardos B, Cohen AL, Fair DA, Power JD, Church JA, Nelson SM, Wig GS, Vogel AC, Lessov-Schlaggar CN, Barnes KA, Dubis JW, Feczko E, Coalson RS, Pruett JR Jr, Barch DM, Petersen SE, Schlaggar BL (2010): Prediction of individual brain maturity using fMRI. Science 329:1358–1361.

Duerden EG, Mak-Fan KM, Taylor MJ, Roberts SW (2012): Regional differences in grey and white matter in children and adults with autism spectrum disorders: An activation likelihood estimate (ALE) meta-analysis. Autism Res 5:49–66.

Fornito A, Yoon J, Zalesky A, Bullmore ET, Carter CS (2011): General and specific functional connectivity disturbances in first-episode schizophrenia during cognitive control performance. Biol Psychiatry 70:64–72.

Fries P (2005): A mechanism for cognitive dynamics: Neuronal communication through neuronal coherence. Trends Cogn Sci 9:474–480.

Fries P (2009): Neuronal gamma-band synchronization as a fundamental process in cortical computation. Annu Rev Neurosci 32:209–224.

Fusar-Poli P, Placentino A, Carletti F, Landi P, Allen P, Surguladze S, Benedetti F, Abbamonte M, Gasparotti R, Barale F, Perez J, McGuire P, Politi P (2009): Functional atlas of emotional faces processing: A voxel-based meta-analysis of 105 functional magnetic resonance imaging studies. J Psychiatry Neurosci 34:418–432.

Geschwind DH, Levitt P (2007): Autism spectrum disorders: Developmental disconnection syndromes. Curr Opin Neurobiol 17:103–111.

Ghanbari Y, Bloy L, Christopher Edgar J, Blaskey L, Verma R, Roberts TL (2013): Joint Analysis of Band-Specific Functional Connectivity and Signal Complexity in Autism. Journal of Autism and Developmental Disorders:1–17.

Greimel E, Nehrkorn B, Schulte-Ruther M, Fink GR, Nickl-Jockschat T, Herpertz-Dahlmann B, Konrad K, Eickhoff SB (2013): Changes in grey matter development in autism spectrum disorder. Brain Struct Funct 218:929–942.

Groen W, Teluij M, Buitelaar J, Tendolkar I (2010): Amygdala and hippocampus enlargement during adolescence in autism. J Am Acad Child Adolesc Psychiatry 49:552–560.

Haber SN (2003): The primate basal ganglia: Parallel and integrative networks. J Chem Neuroanat 26:317–330.

Hagmann P, Sporns O, Madan N, Cammoun L, Pienaar R, Wedeen VJ, Meuli R, Thiran JP, Grant PE (2010): White matter maturation reshapes structural connectivity in the late developing human brain. Proc Natl Acad Sci USA 107:19067–19072.

Havenith MN, Yu S, Biederlack J, Chen N-H, Singer W, Nikolic D (2011): Synchrony makes neurons fire in sequence, and stimulus properties determine who is ahead. J Neurosci 31:8570–8584.

He Y, Wang J, Wang L, Chen ZJ, Yan C, Yang H, Tang H, Zhu C, Gong Q, Zang Y, Evans AC (2009): Uncovering intrinsic modular organization of spontaneous brain activity in humans. PLoS One 4:e5226.

Herbert MR, Ziegler DA, Makris N, Filipek PA, Kemper TL, Normandin JJ, Sanders HA, Kennedy DN, Caviness VS, Jr (2004): Localization of white matter volume increase in autism and developmental language disorder. Ann Neurol 55:530–540.

Hong SB, Zalesky A, Cocchi L, Fornito A, Choi EJ, Kim HH, Suh JE, Kim CD, Kim JW, Yi SH (2013): Decreased functional brain connectivity in adolescents with internet addiction. PLoS One 8:e57831.

Howard MA, Cowell PE, Boucher J, Broks P, Mayes A, Farrant A, Roberts N (2000): Convergent neuroanatomical and behavioural evidence of an amygdala hypothesis of autism. Neuroreport 11:2931–2935.

Hung Y, Smith ML, Bayle DJ, Mills T, Cheyne D, Taylor MJ (2010): Unattended emotional faces elicit early lateralized amygdala-frontal and fusiform activations. Neuroimage 50: 727–733.

Hung Y, Smith ML, Taylor MJ (2012): Development of ACC-amygdala activations in processing unattended fear. Neuroimage 60:545–552.

Ioannides AA, Liu MJ, Liu LC, Bamidis PD, Hellstrand E, Stephan KM (1995): Magnetic field tomography of cortical and deep processes: examples of "real-time mapping" of averaged and single trial MEG signals. Int J Psychophysiol 20:161–175.

Just MA, Cherkassky VL, Keller TA, Minshew NJ (2004): Cortical activation and synchronization during sentence comprehension in high-functioning autism: Evidence of underconnectivity. Brain 127:1811–1821.

Just MA, Keller TA, Malave VL, Kana RK, Varma S (2012): Autism as a neural systems disorder: A theory of frontal-posterior underconnectivity. Neurosci Biobehav Rev 36:1292–1313.

Kaiser J, Lutzenberger W (2005): Human gamma-band activity: A window to cognitive processing. Neuroreport 16:207–211.

Kana RK, Keller TA, Cherkassky VL, Minshew NJ, Just MA (2009): Atypical frontal-posterior synchronization of theory of mind regions in autism during mental state attribution. Soc Neurosci 4:135–52.

Keown CL, Shih P, Nair A, Peterson N, Mulvey ME, Muller RA (2013): Local functional overconnectivity in posterior brain regions is associated with symptom severity in autism spectrum disorders. Cell Rep 5:567–572.

Kesler-West ML, Anderson AH, Smith CD, Avison MJ, Davis CE, Avison RG, Blonder LX (1999): A functional magnetic resonance imaging (FMRI) study of the perception of emotional facial expressions. J Cognitive Neurosci:82.

Kirsch P, Achenbach C, Kirsch M, Heinzmann M, Schienle A, Vaitl D (2003): Cerebellar and hippocampal activation during eyeblink conditioning depends on the experimental paradigm: a MEG study. Neural Plast 10:291–301.

Lachaux JP, Rodriguez E, Martinerie J, Varela FJ (1999): Measuring phase synchrony in brain signals. Hum Brain Mapp 8: 194–208.

Langen M, Schnack HG, Nederveen H, Bos D, Lahuis BE, de Jonge MV, van Engeland H, Durston S (2009): Changes in the developmental trajectories of striatum in autism. Biol Psychiatry 66:327–333.

Lau TM, Gwin JT, McDowell KG, Ferris DP (2012): Weighted phase lag index stability as an artifact resistant measure to detect cognitive EEG activity during locomotion. J Neuroeng Rehabil 9:47.

Li H, Xue Z, Ellmore TM, Frye RE, Wong ST (2014): Network-based analysis reveals stronger local diffusion-based connectivity and different correlations with oral language skills in brains of children with high functioning autism spectrum disorders. Hum Brain Mapp 35:396–413.

Liao W, Qiu C, Gentili C, Walter M, Pan Z, Ding J, Zhang W, Gong Q, Chen H (2010): Altered effective connectivity network of the amygdala in social anxiety disorder: A resting-state fMRI study. Plos One 5:e15238.

Liu L, Ioannides AA, Streit M (1999): Single trial analysis of neurophysiological correlates of the recognition of complex objects and facial expressions of emotion. Brain Topogr 11:291–303.

Lord C, Risi S, Lambrecht L, Cook EH, Leventhal BL, DiLavore PC, Pickles A, Rutter M (2000): The autism diagnostic observation schedule-generic: A standard measure of social and communication deficits associated with the spectrum of autism. J Autism Dev Disord 30:205–223.

Luo Q, Holroyd T, Jones M, Hendler T, Blair J (2007): Neural dynamics for facial threat processing as revealed by gamma band synchronization using MEG. Neuroimage 34:839–847.

Lynall ME, Bassett DS, Kerwin R, McKenna PJ, Kitzbichler M, Muller U, Bullmore E (2010): Functional connectivity and brain networks in schizophrenia. J Neurosci 30:9477–9487.

Lynch CJ, Uddin LQ, Supekar K, Khouzam A, Phillips J, Menon V (2013): Default mode network in childhood autism: Posteromedial cortex heterogeneity and relationship with social deficits. Biol Psychiatry 74:212–219.

Mathewson KJ, Jetha MK, Drmic IE, Bryson SE, Goldberg JO, Schmidt LA (2012): Regional EEG alpha power, coherence, and behavioral symptomatology in autism spectrum disorder. Clin Neurophysiol 123:1798–1809.

McAlonan GM, Cheung V, Cheung C, Suckling J, Lam GY, Tai KS, Yip L, Murphy DG, Chua SE (2005): Mapping the brain in autism. A voxel-based MRI study of volumetric differences and intercorrelations in autism. Brain 128:268–276.

Mills T, Lalancette M, Moses SN, Taylor MJ, Quraan MA (2012): Techniques for detection and localization of weak hippocampal and medial frontal sources using beamformers in MEG. Brain Topogr 25:248–263.

Minshew NJ, Williams DL (2007): The new neurobiology of autism—Cortex, connectivity, and neuronal organization. Arch Neurol 64:945–950.

Minshew NJ, Keller TA (2010): The nature of brain dysfunction in autism: Functional brain imaging studies. Curr Opin Neurol 23:124–130.

Moses SN, Houck JM, Martin T, Hanlon FM, Ryan JD, Thoma RJ, Weisend MP, Jackson EM, Pekkonen E, Tesche CD (2007): Dynamic neural activity recorded from human amygdala during fear conditioning using magnetoencephalography. Brain Res Bull 71:452–460.

Muller RA, Shih P, Keehn B, Deyoe JR, Leyden KM, Shukla DK (2011): Underconnected, but how? A survey of functional connectivity MRI studies in autism spectrum disorders. Cereb Cortex 21:2233–2243.

Murias M, Webb SJ, Greenson J, Dawson G (2007): Resting state cortical connectivity reflected in EEG coherence in individuals with autism. Biol Psychiatry 62:270–273.

Nickl-Jockschat T, Habel U, Michel TM, Manning J, Laird AR, Fox PT, Schneider F, Eickhoff SB (2012): Brain structure anomalies in autism spectrum disorder—a meta-analysis of VBM studies using anatomic likelihood estimation. Hum Brain Mapp 33: 1470–1489.

Nishitani N, Nagamine T, Shibasaki H (1998): Modality-specific subregions in human inferior parietal lobule: a magnetoencephalographic study during cognitive tasks. Neurosci Lett 252: 79–82.

Noesselt T, Driver J, Heinze HJ, Dolan R (2005): Asymmetrical activation in the human brain during processing of fearful faces. Curr Biol 15:424–429.

Orekhova EV, Stroganova TA, Nygren G, Tsetlin MM, Posikera IN, Gillberg C, Elam M (2007): Excess of high frequency electroencephalogram oscillations in boys with autism. Biol Psychiatry 62:1022–1029.

Ortiz E, Stingl K, Muenssinger J, Braun C, Preissl H, Belardinelli P (2012): Weighted phase lag index and graph analysis: Preliminary investigation of functional connectivity during resting state in children. Comput Math Methods Med 2012: 186353.

Palva S, Palva JM (2012): Discovering oscillatory interaction networks with M/EEG: Challenges and breakthroughs. Trends Cognitive Sci 16:219–230.

Palva JM, Monto S, Kulashekhar S, Palva S (2010): Neuronal synchrony reveals working memory networks and predicts individual memory capacity. Proc Natl Acad Sci USA 10716: 7580–7585.

Papanicolaou AC, Pazo-Alvarez P, Castillo EM, Billingsley-Marshall RL, Breier JI, Swank PR, Buchanan S, McManis M, Clear T, Passaro AD (2006): Functional neuroimaging with MEG: normative language profiles. NeuroImage 33:326–342.

Pereda E, Quiroga RQ, Bhattacharya J (2005): Nonlinear multivariate analysis of neurophysiological signals. Prog Neurobiol 77: 1–37.

Pérez Velázquez JL, Galán RF (2013): Information Gain in the Brain's Resting State: A New Perspective on Autism. Frontiers in Neuroinformatics 7:1–10.

Peters JM, Taquet M, Vega C, Jeste SS, Fernandez IS, Tan J, Nelson CA, 3rd, Sahin M, Warfield SK (2013): Brain functional networks in syndromic and non-syndromic autism: A graph theoretical study of EEG connectivity. BMC Med 11:54.

Phillips ML, Drevets WC, Rauch SL, Lane R (2003): Neurobiology of emotion perception I: The neural basis of normal emotion perception. Biol Psychiatry 54:504–514.

Pollonini L, Patidar U, Situ N, Rezaie R, Papanicolaou AC, Zouridakis G (2010): Functional connectivity networks in the autistic and healthy brain assessed using granger causality. Annual International Conference of the IEEE Engineering in Medicine and Biology Society. IEEE Engineering in Medicine and Biology Society, Buenos Aires, Argentina. pp 1730–1733.

Quraan MA, Moses SN, Hung Y, Mills T, Taylor MJ (2011): Detection and localization of hippocampal activity using beamformers with MEG: a detailed investigation using simulations and empirical data. Hum Brain Mapp 32:812–827.

Ramoz N, Reichert JG, Smith CJ, Silverman JM, Bespalova IN, Davis KL, Buxbaum JD (2004): Linkage and association of the mitochondrial aspartate/glutamate carrier SLC25A12 gene with autism. Am J Psychiatry 161:662–669.

Raznahan A, Toro R, Daly E, Robertson D, Murphy C, Deeley Q, Bolton PF, Paus T, Murphy DG (2010): Cortical anatomy in autism spectrum disorder: An in vivo MRI study on the effect of age. Cereb Cortex 20:1332–1340.

Redcay E, Moran JM, Mavros PL, Tager-Flusberg H, Gabrieli JD, Whitfield-Gabrieli S (2013): Intrinsic functional network organization in high-functioning adolescents with autism spectrum disorder. Front Hum Neurosci 7:573.

Riggs L, Moses SN, Bardouille T, Herdman AT, Ross B, Ryan JD (2009): A complementary analytic approach to examining medial temporal lobe sources using magnetoencephalography. Neuroimage 45:627–642.

Rippon G, Brock J, Brown C, Boucher J (2007): Disordered connectivity in the autistic brain: Challenges for the "new psychophysiology". Int J Psychophysiol 63:164–172.

Rizzolatti G, Craighero L (2004): The mirror-neuron system. Annu Rev Neurosci 27:169–192.

Rojas DC, Peterson E, Winterrowd E, Reite ML, Rogers SJ, Tregellas JR (2006): Regional gray matter volumetric changes in autism associated with social and repetitive behavior symptoms. BMC Psychiatry 6:56.

Rojas DC, Teale PD, Maharajh K, Kronberg E, Youngpeter K, Wilson LB, Wallace A, Hepburn S (2011): Transient and steady-state auditory gamma-band responses in first-degree relatives of people with autism spectrum disorder. Mol autism 2:11.

Rubenstein JLR, Merzenich MM (2003): Model of autism: Increased ratio of excitation/inhibition in key neural systems. Genes Brain Behav 2:255–267.

Rubinov M, Sporns O (2010): Complex network measures of brain connectivity: Uses and interpretations. Neuroimage 52:1059–1069.

Schipul SE, Keller TA, Just MA (2011): Inter-regional brain communication and its disturbance in autism. Front Syst Neurosci 5:10.

Schoffelen J-M, Gross J (2009): Source connectivity analysis with MEG and EEG. Hum Brain Mapp 30:1857–1865.

Schumann CM, Hamstra J, Goodlin-Jones BL, Lotspeich LJ, Kwon H, Buonocore MH, Lammers CR, Reiss AL, Amaral DG (2004): The amygdala is enlarged in children but not adolescents with autism; the hippocampus is enlarged at all ages. J Neurosci. 24:6392–6401.

Sparks BF, Friedman SD, Shaw DW, Aylward EH, Echelard D, Artru AA, Maravilla KR, Giedd JN, Munson J, Dawson G, Dager SR (2002): Brain structural abnormalities in young children with autism spectrum disorder. Neurology 59:184–192.

Sporns O, Zwi JD (2004): The small world of the cerebral cortex. Neuroinformatics 2:145–162.

Stam CJ, Nolte G, Daffertshofer A (2007): Phase lag index: Assessment of functional connectivity from multi channel EEG and MEG with diminished bias from common sources. Hum Brain Mapp 28:1178–1193.

Stephen JM, Ranken DM, Aine CJ, Weisend MP, Shih JJ (2005): Differentiability of simulated MEG hippocampal, medial temporal and neocortical temporal epileptic spike activity. J Clin Neurophysiol 22:388–401.

Stigler KA, McDonald BC, Anand A, Saykin AJ, McDougle CJ (2011): Structural and functional magnetic resonance imaging of autism spectrum disorders. Brain Res 1380:146–161.

Streit M, Ioannides AA, Liu L, Wolwer W, Dammers J, Gross J, Gaebel W, Muller-Gartner HW (1999): Neurophysiological correlates of the recognition of facial expressions of emotion as revealed by magnetoencephalography. Brain Res Cogn Brain Res 7:481–491.

Stroganova TA, Orekhova EV, Prokofyev AO, Tsetlin MM, Gratchev VV, Morozov AA, Obukhov YV (2012): High-frequency oscillatory response to illusory contour in typically developing boys and boys with autism spectrum disorders. Cortex 48:701–717.

Supekar K, Menon V, Rubin D, Musen M, Greicius MD (2008): Network analysis of intrinsic functional brain connectivity in Alzheimer's disease. Plos Comput Biol 4:e1000100.

Supekar K, Musen M, Menon V. (2009): Development of large-scale functional brain networks in children. PLoS Biol 7: e1000157.

Supekar K, Uddin LQ, Khouzam A, Phillips J, Gaillard WD, Kenworthy LE, Yerys BE, Vaidya CJ, Menon V (2013): Brain hyperconnectivity in children with autism and its links to social deficits. Cell Rep 5:738–747.

Taylor MJ, Mills T, Pang EW (2011): The development of face recognition; hippocampal and frontal lobe contributions determined with MEG. Brain Topogr 24:261–270.

Tesche CD (1996): Non-invasive imaging of neuronal population dynamics in human thalamus. Brain Res 729:253–258.

Tewarie P, Schoonheim MM, Stam CJ, van der Meer ML, van Dijk BW, Barkhof F, Polman CH, Hillebrand A (2013): Cognitive and clinical dysfunction, altered MEG resting-state networks and thalamic atrophy in multiple sclerosis. PLoS One 8: e69318.

Tsiaras V, Simos PG, Rezaie R, Sheth BR, Garyfallidis E, Castillo EM, Papanicolaou AC (2011): Extracting biomarkers of autism from MEG resting-state functional connectivity networks. Comput Biol Med 41:1166–1177.

Tzourio-Mazoyer N, Landeau B, Papathanassiou D, Crivello F, Etard O, Delcroix N, Mazoyer B, Joliot M (2002): Automated anatomical labeling of activations in SPM using a macroscopic anatomical parcellation of the MNI MRI single-subject brain. Neuroimage 15:273–289.

Uddin LQ, Supekar K, Lynch CJ, Khouzam A, Phillips J, Feinstein C, Ryali S, Menon V (2013): Salience network-based classification and prediction of symptom severity in children with autism. Jama Psychiatry 70:869–879.

Uhlhaas PJ, Singer W (2007): What do disturbances in neural synchrony tell us about autism? Biol Psychiatry 62:190–191.

Uhlhaas PJ, Roux F, Singer W, Haenschel C, Sireteanu R, Rodriguez E (2009): The development of neural synchrony reflects late maturation and restructuring of functional networks in humans. Proc Nat Acad Sci USA 106:9866–9871.

van Dellen E, de Witt Hamer PC, Douw L, Klein M, Heimans JJ, Stam CJ, Reijneveld JC, Hillebrand A (2013): Connectivity in MEG resting-state networks increases after resective surgery for low-grade glioma and correlates with improved cognitive performance. NeuroImage: Clinical 2:1–7.

van Pelt S, Boomsma DI, Fries P (2012): Magnetoencephalography in twins reveals a strong genetic determination of the peak frequency of visually induced gamma-band synchronization. J Neurosci 32:3388–3392.

Vinck M, Oostenveld R, van Wingerden M, Battaglia F, Pennartz CMA (2011): An improved index of phase-synchronization for electrophysiological data in the presence of volume-conduction, noise and sample-size bias. Neuroimage 55:1548–1565.

Vissers ME, X Cohen M, Geurts HM (2012): Brain connectivity and high functioning autism: A promising path of research

that needs refined models, methodological convergence, and stronger behavioral links. Neurosci Biobehav Rev 36: 604–625.

Wallace GL, Dankner N, Kenworthy L, Giedd JN, Martin A (2010): Age-related temporal and parietal cortical thinning in autism spectrum disorders. Brain 133(Pt 12):3745–3754.

Wang X-J (2010): Neurophysiological and computational principles of cortical rhythms in cognition. Physiol Rev 90:1195–1268.

Wang L, Zhu C, He Y, Zang Y, Cao Q, Zhang H, Zhong Q, Wang Y (2009): Altered small-world brain functional networks in children with attention-deficit/hyperactivity disorder. Hum Brain Mapp 30:638–649.

Wechsler D (1999). Wechsler Abbreviated Scale of Intelligence (WASI). San Antonio, TX: Harcourt Assessment.

Werner E, Dawson G, Osterling J, Dinno N (2000): Brief report: Recognition of autism spectrum disorder before one year of age: A retrospective study based on home videotapes. J Autism Dev Disord 30:157–162.

Wetherby AM, Woods J, Allen L, Cleary J, Dickinson H, Lord C (2004): Early indicators of autism spectrum disorders in the second year of life. J Autism Dev Disord 34:473–493.

Williams JHG, Whiten A, Suddendorf T, Perrett DI (2001): Imitation, mirror neurons and autism. Neurosci Biobehav Rev 25: 287–295.

Wilson TW, Rojas DC, Reite ML, Teale PD, Rogers SJ (2007): Children and adolescents with autism exhibit reduced MEG steady-state gamma responses. Biol Psychiatry 62:192–197.

Xia M, Wang J, He Y (2013): BrainNet viewer: A network visualization tool for human brain connectomics. PloS One 8:e68910–e68910.

Yu KK, Cheung C, Chua SE, McAlonan GM (2011): Can Asperger syndrome be distinguished from autism? An anatomic likelihood meta-analysis of MRI studies. J Psychiatry Neurosci 36: 412–421.

Zalesky A, Fornito A, Bullmore ET (2010): Network-based statistic: Identifying differences in brain networks. Neuroimage 53: 1197–1207.